Research Article

Effect of Curing on Mechanical Properties of Cement-Stabilized Coral Sand in Marine Environment

Mingyuan Chen,[1] **Jiuguang Geng**,[1] **Haocheng Xiong**,[2] **Tao Shang**,[1] **Cheng Xue**,[3] **and Montasir Abbas**[4]

[1]*School of Materials Science and Engineering, Chang'an University, Xi'an, China*
[2]*National Center for Materials Service Safety, University of Science and Technology Beijing, Beijing, China*
[3]*CCCC Second Highway Engineering Co. Ltd., Xi'an, China*
[4]*Virginia Tech, Blacksburg, VA, USA*

Correspondence should be addressed to Jiuguang Geng; gengjg@chd.edu.cn

Received 7 May 2020; Revised 23 June 2020; Accepted 29 June 2020; Published 22 July 2020

Academic Editor: Dora Foti

The use of coral sand prepared from cement-stabilized materials can significantly reduce the cost, construction period, and damage to the environment caused by stone mining. The choice of water in mixing and curing the cement-stabilized materials on islands should be considered. Cement-stabilized coral sand was tested in three different preparation and maintenance systems in the marine environment. The compressive strength, weight change, and chloride ion concentration change in cement-stabilized coral sand with different cement content were measured after 7 d, 28 d, 60 d, and 90 d, respectively. The microstructure of specimens was observed by XRD and SEM. Results show that the compressive strength of specimens in the seawater mixing and seawater curing system developed 0.9 MPa faster than that in the fresh water mixing and curing system at an early stage. But the compressive strength of specimens in seawater mixing and seawater curing shrank later, being 0.5 MPa lower than that in fresh water mixing and curing. The cement content was positively correlated with the free chloride ion reaction and mass growth rate. For road construction on islands, the mixing and curing of cement-stabilized coral sand with seawater should be given priority in the early stage.

1. Introduction

Due to the importance of marine exploitation in recent years, infrastructure construction on islands and coastal areas has considerable significance for resource extraction and economic development. The safety and durability of marine engineering have attracted widespread attention. While cement-stabilized material is widely used in road construction on islands and coastal areas [1], the transportation of conventional materials (e.g., gravel and river sand) from inland increases costs, construction periods, and carbon emissions. At the same time, construction using conventional materials requires fresh water which is limited on many islands. Moreover, it is a hotspot that waste materials replace traditional materials at this stage [2, 3], and coral sand is among them. Therefore, when the coral sand accumulated on the beach is available for road subbase construction, the above problems can be reduced to achieve significant economic and environmental benefits [4].

Coral sand is a special type of rock. Its mineral composition is mainly high-magnesium calcite, and the chemical composition is mainly calcium carbonate, an uneven material. Due to its origin and structural characteristics, the road performance of coral sand differs considerably from ordinary sand in compressive strength and durability [5]. Wang et al. observed that coral sand concrete hydration products formed in the pores of coral sand through the transitional zone between coral sand concrete and ordinary river sand concrete. An interlocking structure with the cement matrix is formed, which is conducive to the

development of concrete strength [6]. From the triaxial compression test of coral sand, Coop [7] learned that its critical state is consistent with the main soil characteristics. Geng et al. [8] studied the shear characteristics of coral sand and its interface with the structure. Coral sand had a special shear stress-displacement curve, and with the increase in particle size, the internal friction angle also increased. Since coral sand is a foundation for cement concrete, its use for the base layer is feasible.

In coastal and island areas where fresh water is limited, the use of mixed water will be expensive and work efficiency will be low. Therefore, combining seawater into mixed water can promote the construction of marine structures more efficiently and at a lower cost while reducing excessive use of fresh water resources. Some scholars report that the use of seawater as mixed water in concrete changes the strength of the matrix, due to gains in early strength and shortening solidification times [9, 10]. In addition, due to the chloride ion input, the chemical reaction of C_3S and C_3A was induced to accelerate the hydration process, and the microstructure of the concrete was improved [11]. Adding seawater to the concrete containing the auxiliary cementitious material (SCM) can further improve the pore structure and form a precipitate there [12]. Shi et al. [13] found that a mixed system of metakaolin (MK) and seawater improved the chlorination resistance of concrete by forming a Friedel salt to increase the amount of chemically bound chloride. Li et al. [14] report that concrete mixed with seawater had the highest compressive strength compared with that of the ordinary concrete samples. Pan found that coral sand concrete prepared with seawater and sulfate-resistant cement had good durability and high strength for road construction [15]. Further research on coral concrete showed its applicability to various projects, which promotes the development of materials. Through the dry-wet cycle and sulfate attack test of coral sand concrete, Tang et al. found that loss of the elastic modulus in coral sand concrete was less than that of ordinary concrete [16]. However, seawater contains corrosive compounds [17]. Howdyshell [18] studied the feasibility of using coral as an aggregate in Portland cement concrete, with special attention given to the chloride content that might cause corrosion in structural steel. Zhang et al. [19] studied the effect of salt concentration on the cement-stabilized clay cementing process and found that high-concentration salt had an adverse effect on the unconfined compressive strength of cement-stabilized clay and led to low resistivity. The hydration product is cured in seawater for some time, resulting in excessive Friedel's salt, $Mg(OH)_2$, magnesium silicate hydrate (MSH), $CaCO_3$, etc. This can damage the structure of concrete [20–22]. Due to the limitation of seawater, considering the optimal construction scheme, different maintenance conditions are simulated.

For the cement concrete surface layer of pavement, the paving construction needs no compaction by a road roller. Only mixing well and vibratory compaction is required. The cement stone formed by condensation hardening will bind loose material tightly and give strength to it. However, the amount of cement in cement-stabilized materials is less than that in concrete [23, 24]. Mixing and curing conditions affect the performance of cement-stabilized materials in the marine environment. It can be seen that the researchers used different mixing and curing conditions and the required test methods for different materials construction [25]. This study uses three mixing and curing schemes for cement-stabilized coral sand, mixing and curing with seawater, mixing with fresh water and curing with seawater, mixing and curing with fresh water. The compressive strength, weight change, and chloride ion concentration change were evaluated at different ages. XRD and SEM were used to illustrate the internal structure and composition changes of cement-stabilized coral sand.

2. Materials and Methods

2.1. Materials. The cement used in this study was ordinary Portland cement (P·O 42.5 according to Chinese standard [26]). Its chemical composition and physical properties are shown in Tables 1 and 2, respectively. Natural coral sand required for the trial was taken from Malaysia, whose screening results and basic performance are shown in Tables 3 and 4.

2.2. Curing Plan Design. The Proctor heavy-duty compaction test was performed according to the T0804 method in JTG E51 [27]. The concentration cement used in the tests was 5%, 6%, 7%, and 8% (mass), and five different water contents were selected to perform a compaction test. After mixing, the mixture was placed in a compaction cylinder (Φ100 mm × 127 mm), and then an electric compactor was used to perform compaction in five layers. Each layer was hammered 27 times according to the standard. Dry density and moisture content were recorded, and a curve was drawn to find the optimum moisture content and maximum dry density for different cement contents, as shown in Table 5. The degree of compaction is not less than 97%. The coral sand was then mixed with Portland cement powder before adding water to bring the mixture to the desired water content. The materials were moved into the molds (Φ50 mm × 50 mm) to prepare the stabilized samples for testing.

During the conventional curing process, the scheme was mixed and cured with fresh water. However, fresh water on the island is limited and is expensive to transport from inland. Seawater can be used for curing as an alternative to fresh water. The scheme can be mixed with fresh water and cured with seawater. When seawater is selected to replace the fresh water, seawater mixing and seawater curing scheme were used in the marine environment. The specimens were shaped and cured according to the three schemes in Table 6. To achieve a similar condition to the seawater in the South China Sea, sea salt was prepared [28]. For the main chemical components, Cl^- was 11.76 g, Mg^{2+} 1.84 g, and SO_4^{2-} 1.53 g per 1 L seawater. The concentration of artificial seawater is about 20 g/L, and in order to compare the effects of different seawater concentrations on compressive strength, the seawater concentration was 10 g/L, 20 g/L, and 30 g/L,

Table 1: Chemical analysis of the cement (wt%).

Components	SiO_2	Al_2O_3	CaO	Fe_2O_3	MgO	K_2O	Na_2O	SO_3
	22.61	5.94	63.72	3.22	1.98	0.39	0.12	1.99

Table 2: Physical properties of the cement.

Setting time (min)		Flexural strength (MPa)		Compressive strength (MPa)	
Initial	Final	7 d	28 d	7 d	28 d
92	220	4.7	8.9	33.7	43.2

Table 3: Screening results of coral sand.

Sieve size (mm)	9.5	4.75	2.36	1.18	0.6	0.3	0.15	0.075
Through rate (%)	100	93.9	87.3	71.3	53.8	27.3	10.5	0.03

Table 4: Basic performance of coral sand.

Apparent density (g/cm^3)	Bulk density (g/cm^3)	Water absorption (%)	Sand equivalent (%)	Rugged (%)	Methylene blue value
2.626	1.287	15.8	71.8	2.37	1.25

Table 5: The optimum water content and the maximum dry density.

Cement content (%)	The optimum water content (%)	The maximum dry density (g/cm^3)
5.0	10.1	1.689
6.0	10.4	1.698
7.0	10.7	1.712
8.0	11.2	1.729

Table 6: Shaping and curing scheme.

Mixing	Immersion curing	Abbreviation
Seawater	Seawater	SS
Fresh water	Seawater	FS
Fresh water	Fresh water	FF

respectively. After casting, the specimens were cured with fresh water and artificial seawater, respectively, in a moist room (temperature 20 ± 1°C and RH 100%). For all specimens, the compressive strength, free chloride content, and weight were measured.

2.3. Compressive Strength Test. The unconfined compressive strength (UCS) of specimens was tested using a microcomputer control electronic universal testing machine (CMT5105) and referred to a standard for inorganic binder stabilized material test method (JTG/T 0805) [27]. Six samples were investigated for each age and then averaged with the coefficient of variation ≤6%. The loading rate is 1 mm/min. After the specimen was damaged, the failure strength (F) was recorded. The n-day unconfined compressive strength (C_n) was calculated using equation (1), where n is 7°d, 28°d, 60°d, 90°d, and 180°d.

$$C_n = \frac{F}{S}. \tag{1}$$

To compare the unconfined compressive strength in different mixing and curing schemes, the change of the n-day UCS compared with that of the 7-day UCS (R_7) and 60-day UCS (R_{60}) was calculated using the following equations:

$$R_7 = \frac{C_n - C_7}{C_7}, \tag{2}$$

$$R_{60} = \frac{C_n - C_{60}}{C_{60}}. \tag{3}$$

2.4. Weight Change Test. The weight of specimens after immersion in seawater and fresh water was measured, and the surface of the specimen was dried by a wet towel before measurement. The initial mass (m_0) was the mass of specimens after absorbing saturated water on the first day of curing. Then, the mass (m_t) of the specimens after curing for different days was measured. And, the weight was measured with an accuracy of 0.01 g. The weight change (W) was calculated using equation (4), where t is 7 d, 28 d, and 90 d:

$$W = \frac{m_t - m_0}{m_0} \times 100\%. \tag{4}$$

2.5. Chloride Content Test. After the specimens had been kept in seawater and fresh water for 28 days, 90 days, and 180 days, the free chloride content of the solution was measured. Specimens with approximately 100 g solution were prepared. The amount of free chloride ion was measured by water-soluble according to ASTM C1218 [29].

2.6. SEM Analysis. The microstructure of main hydration products of cement-stabilized coral sand in the system was performed using SEM (Hitachi S-4800). The specimens were prepared according to the following procedure: we collected some broken pieces from each curing age and soaked them in anhydrous ethanol for a week to stop their hydration. Then, the collected pieces were dried in vacuum at 45°C for 24 h and gold films were deposited on them. The samples were then scanned under 1,000x~10,000x magnification, and the fracture surface morphology information of cement-stabilized coral sand samples at different curing time was obtained.

2.7. XRD Analysis. XRD (AXS D8 ADVANCE) was used to determine the composition of the reaction products by identifying specific diffraction peaks for different substances. The specimens were prepared with similar procedures of SEM analysis. Samples were ground into powder with a particle size smaller than 0.08 mm. After curing and drying, they were ground into a powder and then placed in a sample cell (Φ10 mm × 1 mm). The diffraction angle was set from 10° to 70° for testing.

3. Results and Discussion

3.1. Unconfined Compressive Strength. The unconfined compressive strength of cement-stabilized material is the basic property in all indices. Figure 1(a) shows the unconfined compressive strength of samples mixed with seawater and cured in seawater immersion (SS scheme) for different curing times. From the results, the early strength of seawater-mixed coral sands was developed rapidly. The UCS of the sample at 7 d could reach 85.6% of the sample at 28 d, but late strength developed slowly, even with a slight decrease of 5~8% after 60 days. The strength remained similar after 180 days. Usually, more hydration products will be obtained with higher cement content, and the ability to combine with chloride ions will be stronger, resulting in a lower effect of seawater corrosion by the formation of chloroaluminate (Friedel's salt) [30, 31]. Although the UCS values were decreased in the later period, the UCS values of cement-stabilized coral sand with cement contents of 6%, 7%, and 8% after 7 days curing meet the requirements of the Technical Guidelines for Construction of Highway Roadbases (JTG/T F20-2015) for the subbase layer strength (2.5~4.5 MPa) of the heavy traffic expressway.

The unconfined compressive strength of samples which were mixed with fresh water and cured in seawater immersion (FS scheme) in different curing times is shown in Figure 1(b). Compared with Figure 1(a), it can be seen that the initial strength of SS was slightly higher than that of FS under the same cement dosage, but the long-term strength was lower than that of SS. Because the concentration of Cl^- was lower in the FS scheme, initial catalysis of Cl^- was not obvious and the early strength was no more sufficient than in the SS scheme. However, late strength gradually decreased by 3.5~5.5% after 60 days although it was much smaller than in the SS scheme. Therefore, it can be explained that the negative impact of seawater immersion in the FS scheme was smaller than in the SS scheme.

Figure 1(c) shows the unconfined compressive strength of samples mixed with fresh water and cured in fresh water immersion (FF scheme) at different curing times. Compared with the compressive strength in Figures 1(a) and 1(b), it can be analyzed that the UCS of FF was the smallest at curing on 7 d and 28 d (about 2.0~2.5 MPa), but it continued to increase and surpassed that of SS and FS after 60 days. When the curing time reached 180 d, the rate of strength slowed down. Since there was no Cl^- in catalytic effect in the early stage and negative impact in the long-term stage, the compressive strength continued to increase. After 90 days, the degree of cement hydration was already high, so the compressive strength scarcely increased.

The change rate of UCS with different cement contents at different curing times was compared with those at 7 d and 60 d as shown in Table 7. The growth rate of the compressive strength of FS gradually decreased with the increase in curing time. The maximum value is 46.0%. The same growth pattern occurred in the compressive strength growth rate of SS (the maximum reached 31.4%), but the decay rate was faster than that of FS. In the SS scheme, the concentration of chloride ions was high since the samples were mixed with seawater and cured in seawater immersion, so the degree of erosion in the long-term stage was severe. Compared with the UCS at 60 d, the UCS reduction rate of cement-stabilized coral sand with 5% cement content was 9.5% at 180 d. The growth rate of FF's UCS continued to increase and then remained similar. However, there was no tendency to decay because there was no seawater erosion. When it reached 180 d, the growth rate of compressive strength reached over 70%.

Simultaneously, considering the effect of seawater concentration on hydration products and erosion, the UCS of specimens was evaluated with 7% cement content cured at different seawater concentrations (10 g/L, 20 g/L, and 30 g/L) for 28 days, 60 days, 90 days, and 180 days, as shown in Figure 2. It can be concluded that as the seawater concentration increased, the early strength increased, reaching 3.5 MPa at 7 days, because the chloride ion concentration promoted early strength. However, after 60 days, with the concentration of seawater increasing, the UCS decreased more rapidly because seawater erosion affected the overall structure. The UCS of specimens cured in seawater at 30 g/L concentration decreased by 7.5% more than with 10 g/L. The more salt in the seawater, the more Friedel's salt was in the hydration product. Although microexpansion filled the pores, excessive Friedel's salt caused microcracks.

Figure 3 displays two symmetrical cross-sectional views of the sample after strength testing. From Figure 3(a), it can

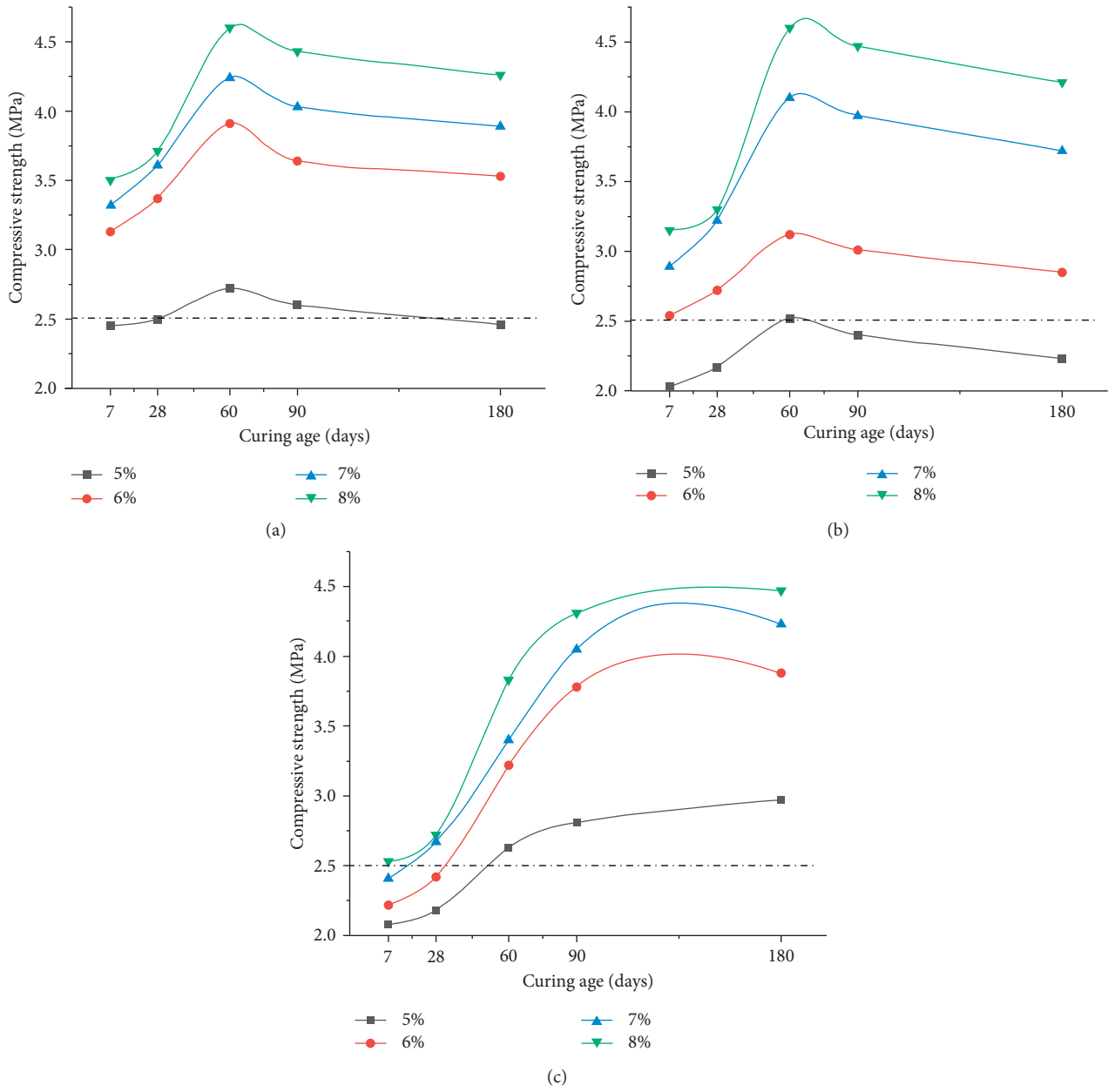

Figure 1: The unconfined compressive strength in different schemes. (a) The mixing and curing with seawater scheme (SS). (b) The mixing with fresh water and curing with seawater scheme (FS). (c) The mixing and curing with fresh water scheme (FF).

Table 7: Change of the compressive strength (%).

Curing time (d)		SS				FS				FF			
		5%	6%	7%	8%	5%	6%	7%	8%	5%	6%	7%	8%
Compared with 7 d (R_7)	28	2.0	7.7	8.7	6.0	6.9	7.1	11.4	4.8	4.8	9.0	10.8	7.5
	60	11.0	24.9	27.7	31.4	24.1	22.8	41.9	46.0	26.4	45.1	41.1	51.4
Compared with 60 d (R_{60})	90	−4.4	−6.9	−4.9	−3.7	−4.7	−3.5	−3.2	−2.8	6.8	17.4	19.1	12.5
	180	−9.5	−9.7	−8.3	−7.4	−11.5	−8.0	−9.3	−8.5	12.9	20.5	24.4	16.7

be seen that, after the ultimate pressure of the coral sand, cracks were generated from the inside of the sand and the sand fractured to cause a significant macroscopic intensity. Figure 3(b) shows that, after pressure was applied, cracks occurred from the interfacial transition zone between the cement and the coral sand, so the entire coral sand particle could be seen from the profile. Overall, cracks appeared more frequently from the interior of the coral sand than

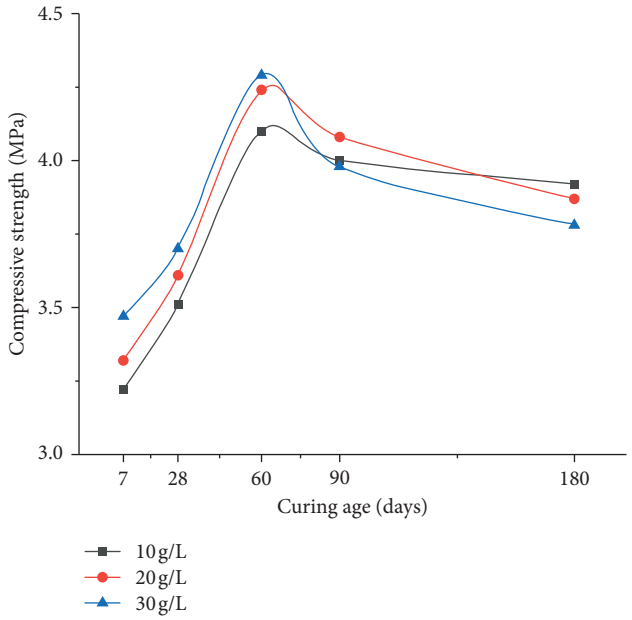

Figure 2: Compressive strength of 7% scheme in different seawater contents.

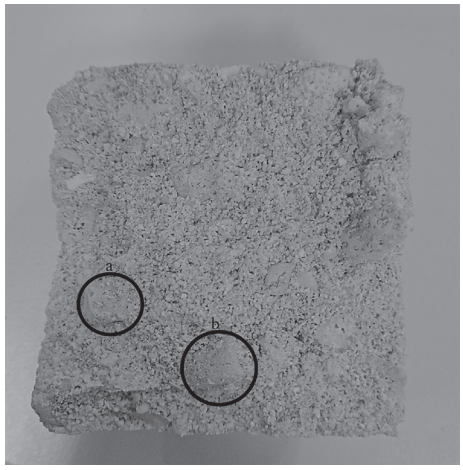

Figure 3: Schematic diagram of the sample: (a) broken particles; (b) complete particles.

from the interface transition zone. The reason for producing the compressive strength was mainly that the cement hydrates to form a whole and was supported by the coral sand skeleton structure.

3.2. Weight Change. For all cement-based materials, as the hydration reaction occurs, the mass of the specimens will increase or decrease, which is a comprehensive process [10]. The increase is mainly due to the formation of hydration products, the absorption of water in coral sand, and the crystallization of salts in pores. On the other hand, since samples were cured in water, the man-made operation caused corner defects and errors in mass reduction. This paper studied the comparison of theoretical values (referred to as T) and actual values (referred to as F) of mass change. In the calculation of the theoretical value, the growth rate of cement hydration heat was related to age, in which on 7 d, there was 70% hydration heat, on 28 d, 89% hydration heat, and on 90 d, 96% hydration heat [15]. This study theoretically calculated them according to the maximum value of hydration products. According to the DSC curve [10], under the drying condition of 100°C–200°C, only AFt had no bound water, and $Ca(OH)_2$ and C-S-H were not dehydrated. The initial mass (m_0) is the average of the samples' initial mass. The main chemical formulas are

$$C_3S + H_2O \longrightarrow C-S-H + Ca(OH)_2 \quad (5)$$

$$C_2S + H_2O \longrightarrow C-S-H + Ca(OH)_2 \quad (6)$$

$$C_3A + Ca(OH)_2 + Cl- + H_2O \longrightarrow C_3A \cdot CaCl_2 \cdot 10H_2O \quad (7)$$

Figure 4 compares the theoretical and actual values at different schemes at 5% and 8% cement content, respectively. From Figure 4(a), it can be observed that, as the age increased, the quality of the samples with 5% cement content grew faster at first and then slower, and the theoretical value was always larger than the actual value. Although the effect of hydration caused the mass to increase, the micro-dissolution of the hydration product and the loss of the corners of the samples caused the value of the mass change to be smaller than the theoretical value although there was little difference between theoretical and actual values. From Figure 4(b), it can be observed that the actual value of the sample weight change at 8% cement content was less than the theoretical value at 28 d but exceeded the theoretical value after 90 d. The SS scheme had the fastest increase rate in quality in seawater conservation and increased by 0.69% in the 90 days. The reasons for this rapid increase were presumed to be the formation of high hydration products of cement content, water absorption during hydration, and formation of Friedel's salt [32]. Furthermore, combining the two figures shows that the weight change of the specimens at 8% cement content was generally 0.1~0.2% larger than that of 5% cement content: more hydration products are produced during curing with more cement content, causing an increase in quality.

In the comparison of the weight changes in the three systems, it can be found that the mass in the SS scheme had the fastest growth rate, followed by that in the FS and FF schemes. The early mass growth in the SS scheme was rapid, with a general growth rate of 0.05~0.1%. The concentration of chloride ions affected the amount of $C_3A{\cdot}CaCl_2{\cdot}10H_2O$ produced during the hydration reaction and was a principal reason for the increase in quality. The hydration products in the SS scheme included C-S-H, Aft, and $C_3A{\cdot}CaCl_2{\cdot}10H_2O$. The hydrated products in FS scheme included C-S-H, Aft. and a small amount of $C_3A{\cdot}CaCl_2{\cdot}10H_2O$, while there was no $C_3A{\cdot}CaCl_2{\cdot}10H_2O$ found in FF scheme. These products included or absorbed considerable water. In addition, salt was found to be attached to the surface of the pore wall and added weight within the pore.

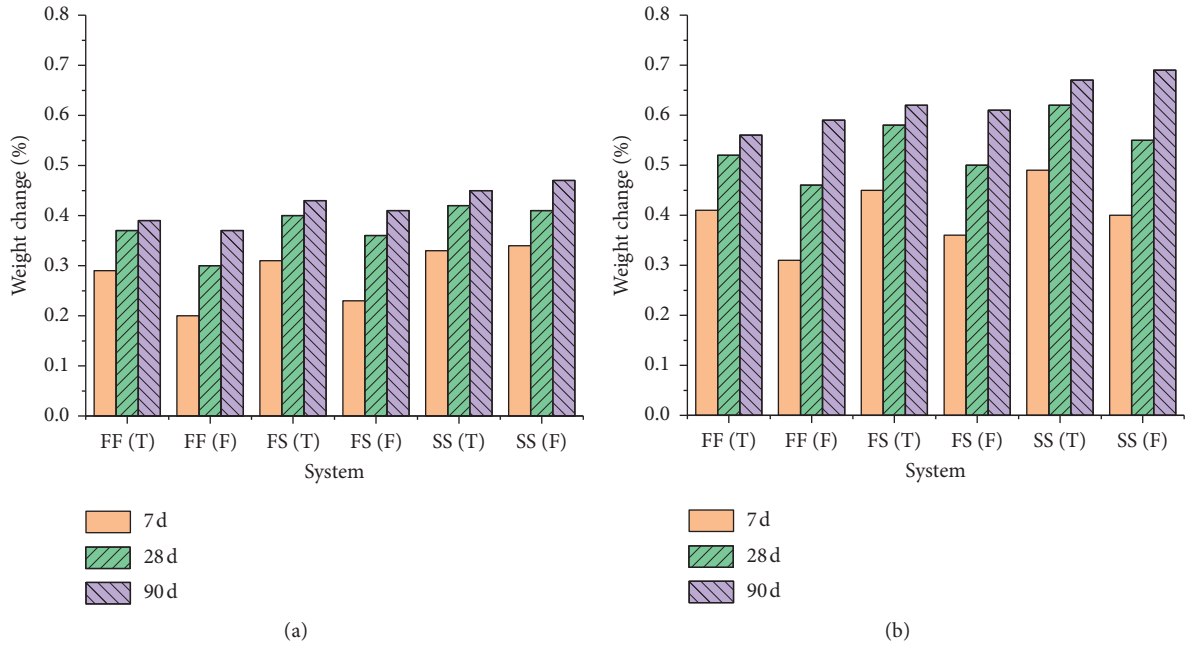

Figure 4: Weight changes of different cement content systems. (a) 5% cement content systems. (b) 8% cement content systems.

3.3. Chloride Content. Chloride binding is the reaction between free chloride, C_3A, and $Ca(OH)_2$ in the systems to produce chloroaluminate compounds—Friedel's salt (equation (7)). Therefore, the reaction of free chloride ions caused an increase in chloride binding. Figure 5 shows the free chloride contents reduction rate of different cement contents immersed in seawater at different ages. The free chloride content of pure coral sand (aggregate without any processing) and samples at different cement contents and different ages in the FF system are shown in Table 7. The chloride ion concentration in seawater alone was 11.76 g/L.

As shown in Figure 5, after immersion in seawater, the higher the cement content, the stronger the ability of the hydration product to bind chloride ions (that of 8% cement content is 0.6% which is more than that of 5% cement content). Second, regardless of the cement content, the chloride ion content of the immersion solution decreased rapidly with age (7 d to 90 d) before reaching a stable stage. From 28 d to 90 d, the free chloride ion decreased by only 0.2%, indicating that the hydration reaction was relatively sufficient. The filling of Friedel's salt and the effect of accelerating pozzolanic activity enhanced the overall compactness and hindered the entry of free chloride ions in seawater. Simultaneously, the coral sand solidified some free chloride ions, reduced the free chlorine content of the solution, and increased the quality of the sample. The free chloride ion in the FS scheme was much faster than that in the SS scheme because FS had no free chloride ions when forming the samples, and there was a rapid free chloride ion reaction in seawater immersion.

For the FF scheme, different results were obtained compared with that for the FS and SS schemes. As shown in Table 8, pure coral sand could precipitate a small number of free chloride ions (0.156 g/L) in the case of fresh water soaking. As expected, there was a trace of chloride ions in the coral sand. The samples in the FF scheme were similar to the pure coral sand solution test concentrations—only about 0.005 g/L free chloride ions were reduced. This indicated

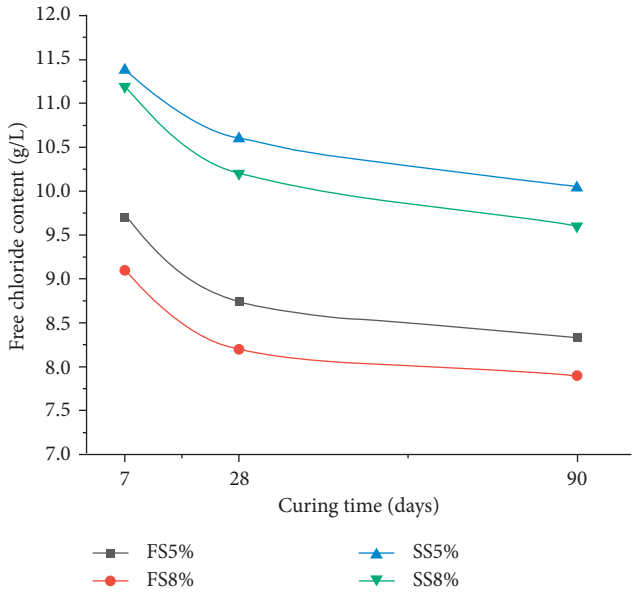

Figure 5: Free chloride content reduction rate in FS and SS systems.

Table 8: Free chloride content in fresh water (g/L).

	7 d	28 d	90 d
Pure coral sand	0.156	0.156	0.156
FF 5%	0.144	0.138	0.132
FF 8%	0.134	0.127	0.123

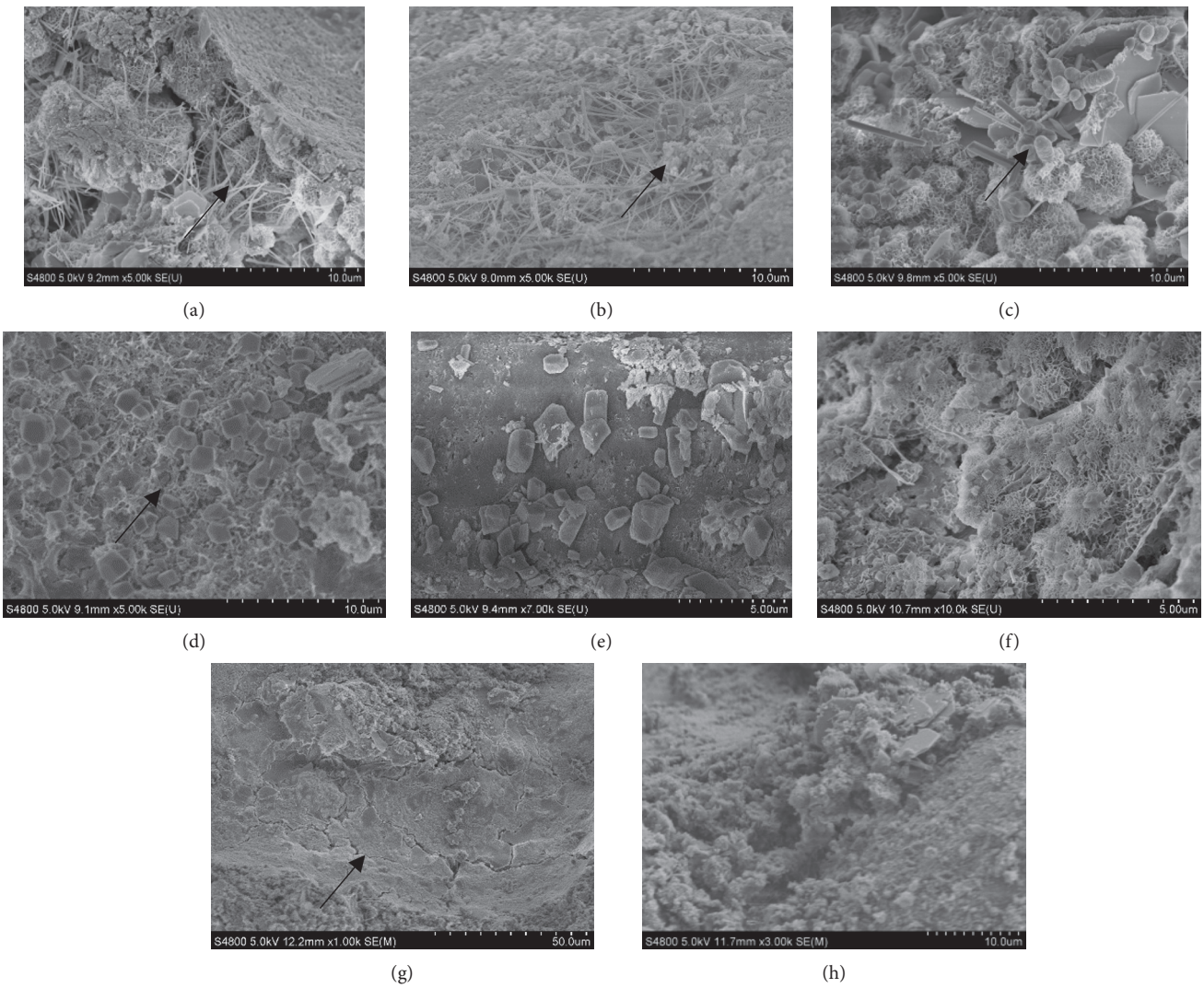

Figure 6: SEM images of cement-stabilized sand in different curing schemes. (a) 7 d-SS8%; (b) 28 d-SS8%; (c) 60 d-SS8%; (d) 28 d-SS7%; (e) 28 d-FS7%; (f) 28 d-FF7%; (g) 60 d-FS8%; (h) 7 d-FF8%.

that, in the FF scheme, there was no Friedel's salt. It was even possible that the hydration product was more easily dissolved due to ion exchange, and the pores were increased [33]. The quality of the FF system had also shown the slowest growth based on previous quality changes.

3.4. SEM Analysis. As known, SEM has the characteristics of simple sample preparation, high resolution, and strong stereoscopic effect. In the three systems, the samples were scanned to obtain the surface morphology and interface transition zone of cement-stabilized coral sand at different ages to observe the main hydration products of cement-stabilized coral sand.

From Figure 6(a), long rod-shaped AFt was interlaced with the flocculent C-S-H gel in the interfacial transition zone at 7 d after hydration of all the cement-stabilized coral sand materials in the SS system. These were in close contact with the coral sand interface. Filling the internal pores and increasing compactness were conducive to early strength development. AFt and C-S-H were formed more when the hydration age reached 28 days and with the formation of Friedel's salt, as shown in Figure 6(b). Figure 6(c) shows that AFt had grown thicker at 60 days of hydration and a large number of flocculent C-S-H intercalated with AFt and $Ca(OH)_2$ formed an overall dense structure.

Figures 6(d)~6(f) are comparisons of samples of the same cement content at the same age for the three systems. As shown, at 28 d, there were some Friedel's salt particles formed on the specimen in the SS system, a small amount in the FS system, and nothing in the FF system. Friedel's salt precipitates in the pore solution plug the pores and improve the pore size distribution, rendering it denser and thereby increasing the early strength. Therefore, the order of compressive strength at this time from large to small was SS, FS, and FF. When the age was less than 60 days (Figure 6(g)), microcracks began to appear in the SS and FS systems due to crystallization pressure of excessive Friedel's salt, which

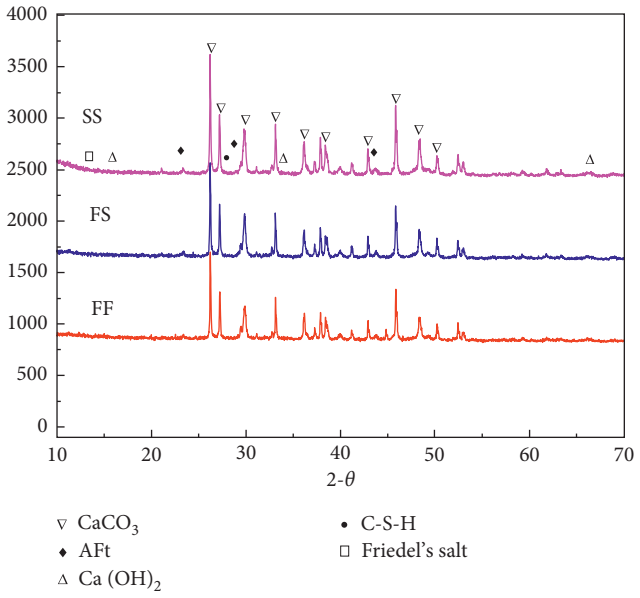

Figure 7: XRD pattern of 60-day cement-stabilized coral sand.

reduced late strength and showed a retraction phenomenon [34, 35]. There were no microcracks in the FF system, and the strength increased and finally exceeded that in the SS and FS systems.

As shown in Figure 6(h), curing at 7 days in the FF system, $Ca(OH)_2$ adhered to the coral sand interface and filled pores. However, only a small amount of C-S-H gel and AFt was observed, and early strength developed slowly. With the increase of hydration time, a large number of irregularly shaped $Ca(OH)_2$ interacted with C-S-H gel and AFt, the overall structure became more compact, and the strength continued to increase in the later period.

3.5. XRD Analysis. Together with the compressive strength tests, the weight change tests, and the chloride content tests, XRD is used to identify the crystal product of cement-stabilized coral sand during solidification and illustrate the effect of mineral production on the properties of cement-stabilized coral sand mixed with seawater [36]. XRD patterns of the sample with 8% cement content (SS, FS, and FF schemes) cured at 60 d at 10–70° were recorded. As shown in Figure 7, the hydration product types were essentially the same in three curing schemes. The main hydration products are $Ca(OH)_2$, C-S-H, and AFt. Among them, the diffraction intensity of calcite was obvious, and it was the main component of coral sand. It did not react with clinker minerals in Portland cement. In the range of 35–40°, there was a weak diffraction peak of $Ca(OH)_2$, because, by 60 d, $Ca(OH)_2$ had almost completely reacted to generate $C_3A{\cdot}CaCl_2{\cdot}10H_2O$, and some of it got dissolved in water. In the 25–30° range, C-S-H was a colloidal size crystal and tended to have a low degree of crystallinity. Therefore, in the XRD pattern, the diffraction peak was extremely weak and easily masked by other peaks. There were obvious AFt diffraction peaks at multiple angles, which was one of the main sources of compressive strength of the system. In the range of 10–15°, $C_3A{\cdot}CaCl_2{\cdot}10H_2O$ had peaked, among which the SS peak was the highest and the FF had nothing. Although $C_3A{\cdot}CaCl_2{\cdot}10H_2O$ can improve the compressive strength and improve the compactness between cement and coral sand, it needs to be combined with chloride ions to do so.

4. Conclusions

Coral sand is particularly important in the construction and development of island infrastructure. According to different curing conditions, a shortage of aggregates and fresh water resources can be alleviated in marine environments. Based on the test results, the following conclusions can be drawn:

(1) In the three systems, the early strength of cement-stabilized coral sand with seawater mixing and curing was 0.9 MPa which is more than that with fresh water mixing and curing, but late strength was 0.5 MPa lower than that with fresh water mixing and curing. In the case of seawater curing, compressive strength decreased after 60 days, mainly due to the generation of microcracks and ion exchange.

(2) The UCS at 7 d of cement-stabilized coral sand with 6% cement content in the SS scheme can meet the base requirements in the guidelines JTG/T F20-2015 and road design. When cement-stabilized coral sand is used for the subbase, the cement content of 6% is sufficient in the SS and FS schemes. This provides for the possibility of its application in road infrastructure construction in islands and coastal areas.

(3) Observing the cement-stabilized coral sand microstructure, it was found that the cement hydration products formed in the coral sand holes and rough interfaces and the mechanical bite of the coral sand are conducive to the stability of the cement to stabilize the formation of coral sand.

(4) As age increased, the sample's mass gradually increased but was generally lower than the theoretical value of the mass change. There was a formation of hydration products and Friedel's salt. The more the cement content, the easier it is to combine with free chloride ions in the solution.

Data Availability

Some of the data required to reproduce these findings cannot be shared at this time as the data also form part of an ongoing study.

Conflicts of Interest

The authors declare that there are no conflicts of interest regarding the publication of this paper.

Acknowledgments

This research was supported by the Fundamental Research Funds for the Central Colleges (310831173701), the National Natural Science Foundation of China (51608045), the

National Key R&D Program of China (2017YFB0309903-02), and the Chinese Post-doctoral Science Foundation (2015M582590).

References

[1] R. A. Arumugam and K. Ramamurthy, "Study of compressive strength characteristics of coral aggregate concrete," *Magazine of Concrete Research*, vol. 48, no. 9, pp. 141–148, 1996.

[2] D. Foti, M. Lerna, M. F. Sabbà et al., "Mechanical characteristics and water absorption properties of blast-furnace slag concretes with fly ashes or microsilica additions," *Applied Sciences*, vol. 9, no. 7, 2019.

[3] D. Foti and D. Cavallo, "Mechanical behavior of concretes made with non-conventional organic origin calcareous aggregates," *Construction and Building Materials*, vol. 179, pp. 100–106, 2018.

[4] S. Zhang, *Experimental Study on the Fatigue Property and Microscopic Mechanism of Coral Concrete*, Guangxi University, Nanning, China, 2012.

[5] H. Yu, Z. Sun, and C. Tang, "Physical and mechanical properties of CRS in the nansha islands," *Marine Science Bulletin*, vol. 2, pp. 31–39, 2006.

[6] Q. Wang, P. Li, Y. Tian, W. Chen, and C. Su, "Mechanical properties and microstructure of Portland cement concrete prepared with coral reef sand," *Journal of Wuhan University of Technology (Materials Science)*, vol. 31, no. 5, pp. 996–1001, 2016.

[7] M. R. Coop, "The mechanics of uncemented carbonate sands," *Géotechnique*, vol. 40, no. 4, pp. 607–626, 1990.

[8] Y. Geng, Y. Lu, F. Li et al., "Experimental analysis of shear properties of coral sands," *Journal of PLA University of Science and Technology (Natural Science Edition)*, vol. 18, no. 1, pp. 29–36, 2017.

[9] T. Nishida, N. Otsuki, H. Ohara et al., "Some considerations for applicability of seawater as mixing water in concrete," *Journal of Materials in Civil Engineering*, vol. 27, no. 7, 2015.

[10] G. Li, A. Zhang, Z. Song, C. Shi, Y. Wang, and J. Zhang, "Study on the resistance to seawater corrosion of the cementitious systems containing ordinary Portland cement or/and calcium aluminate cement," *Construction and Building Materials*, vol. 157, pp. 852–859, 2017.

[11] T. U. Mohammed, H. Hamada, and T. Yamaji, "Performance of seawater-mixed concrete in the tidal environment," *Cement and Concrete Research*, vol. 34, pp. 593–601, 2005.

[12] N. Otsuki, T. Saito, and Y. Tadokoro, "Possibility of sea water as mixing water in concrete," *Journal of Civil Engineering and Architecture*, vol. 6, pp. 1273–1279, 2017.

[13] Z. Shi, Z. Shui, Q. Li, and H. Geng, "Combined effect of metakaolin and sea water on performance and microstructures of concrete," *Construction and Building Materials*, vol. 74, pp. 57–64, 2015.

[14] Q. Li, H. Geng, Y. Huang, and Z. Shui, "Chloride resistance of concrete with metakaolin addition and seawater mixing: a comparative study," *Construction and Building Materials*, vol. 101, pp. 184–192, 2015.

[15] B. Pan and W. Zhuobin, "Experimental study on effects to CRS concrete compressive strength of raw materials," *Engineering Mechanics*, vol. 1, pp. 221–225, 2015.

[16] J. Tang, H. Cheng, Q. Zhang et al., "Development of properties and microstructure of concrete with coral reef sand under sulphate attack and drying-wetting cycles," *Construction and Building Materials*, vol. 165, pp. 647–654, 2018.

[17] J. Xiao, C. Qiang, A. Nanni et al., "Use of sea-sand and seawater in concrete construction: current status and future opportunities," *Construction and Building Materials*, vol. 155, pp. 1101–1111, 2017.

[18] Howdyshell, *The Use of Coral as Aggregate and Cement Concrete Structures*, Army Construction Engineering Research Laboratory, Champaign, IL, USA, 1974.

[19] D. Zhang, Z. Cao, L. Fan, S. Liu, and W. Liu, "Evaluation of the influence of salt concentration on cement stabilized clay by electrical resistivity measurement method," *Engineering Geology*, vol. 170, pp. 80–88, 2014.

[20] K. De Weerdt, H. Justnes, and M. R. Geiker, "Changes in the phase assemblage of concrete exposed to sea water," *Cement and Concrete Composites*, vol. 47, pp. 53–63, 2014.

[21] A. Guerrero, S. Goñi, and V. R. Allegro, "Effect of temperature on the durability of class C fly ash belite cement in simulated radioactive liquid waste: synergy of chloride and sulphate ions," *Journal of Hazardous Materials*, vol. 165, no. 1–3, pp. 903–908, 2009.

[22] Q. Yuan, C. Shi, G. De Schutter, K. Audenaert, and D. Deng, "Chloride binding of cement-based materials subjected to external chloride environment-a review," *Construction and Building Materials*, vol. 23, no. 1, pp. 1–13, 2009.

[23] G. Qian, T. Huang, and S. Bai, "Use of cement-stabilized granite mill tailings as pavement subbase," *Journal of Materials in Civil Engineering*, vol. 23, no. 11, pp. 1575–1578, 2011.

[24] X. Liang and W. Yu, "Optimum mixture ratio of cement and red mud stabilized graded crushed stones based on grey situation decision," *Advanced Materials Research*, vol. 602–604, pp. 968–971, 2012.

[25] Z. Li and Y. Chen, "Test and analysis of properties for different types of semi-rigid base materials," *Journal of Chang'an University (Natural Science Edition)*, vol. 32, pp. 41–46, 2012.

[26] JTG/T F20, *Technical Guidelines for Construction of Highway Roadbases," Standard*, Ministry of Transport of the People's Republic of China, Beijing, China, 2015.

[27] JTG/T E51, *Test Methods of Materials Stabilized with Inorganic Binders for Highway Engineering*, Ministry of Transport of the People's Republic of China, Beijing, China, 2009.

[28] Z. Li, S. Feng, C. Su et al., "Seawater chemical composition erodes cement-based materials," *Concrete*, vol. 5, pp. 8–11, 2012.

[29] Q. Li, J. Chen, Q. Shi, and S. Zhao, "Macroscopic and microscopic mechanisms of cement-stabilized soft clay mixed with seawater by adding ultrafine silica fume," *Advances in Materials Science and Engineering*, vol. 2014, pp. 1–12, 2014.

[30] M. V. A. Florea and H. J. H. Brouwers, "Chloride binding related to hydration products," *Cement and Concrete Research*, vol. 42, no. 2, pp. 282–290, 2012.

[31] B. Ma, C. Li, H. Tan et al., "Effect of styrene-acrylate-emulsion on chloride binding capacity in cement-based materials," *Bulletin of the Chinese Ceramic Society*, vol. 38, no. 1, pp. 200–204, 2019.

[32] S. Cheng, Z. Shui, T. Sun, R. Yu, and G. Zhang, "Durability and microstructure of coral sand concrete incorporating supplementary cementitious materials," *Construction and Building Materials*, vol. 171, pp. 44–53, 2018.

[33] X. Wang, R. Yu, Z. Shui, Q. Song, and Z. Zhang, "Mix design and characteristics evaluation of an eco-friendly Ultra-High Performance Concrete incorporating recycled coral based materials," *Journal of Cleaner Production*, vol. 165, pp. 70–80, 2017.

[34] C. Qiao, P. Suraneni, and J. Weiss, "Damage in cement pastes exposed to NaCl solutions," *Construction and Building Materials*, vol. 171, pp. 120–127, 2018.

[35] Z. Shi, M. R. Geiker, B. Lothenbach et al., "Friedel's salt profiles from thermogravimetric analysis and thermodynamic modelling of Portland cement-based mortars exposed to sodium chloride solution," *Cement and Concrete Composites*, vol. 78, pp. 73–83, 2017.

[36] W. E. Tabet, A. B. Cerato, S. Andrew, and E. Madden, "Characterization of hydration products' formation and strength development in cement-stabilized kaolinite using TG and XRD," *Journal of Materials in Civil Engineering*, vol. 30, no. 10, pp. 1–11, 2018.